

Observation of a two-dimensional electron gas at the surface of annealed SrTiO₃ single crystals by scanning tunneling spectroscopy

R. Di Capua,^{1,2,*} M. Radovic,^{1,3,†} G. M. De Luca,¹ I. Maggio-Aprile,⁴ F. Miletto Granozio,¹ N. C. Plumb,⁵ Z. Ristic,^{1,4} U. Scotti di Uccio,^{1,6} R. Vaglio,^{1,6} and M. Salluzzo¹

¹CNR-SPIN, Complesso Universitario Monte S. Angelo, Via Cintia I-80126 Napoli, Italy

²Dipartimento S.p.e.S., Università degli Studi del Molise, Via De Sanctis I-86100 Campobasso, Italy

³Institut de la Matière Complexe, EPF Lausanne, CH-1015 Lausanne, Switzerland

⁴Département de Physique de la Matière Condensée, University of Geneva, 24 Quai Ernest-Ansermet, CH-1211 Geneva 4, Switzerland

⁵Swiss Light Source, Paul Scherrer Institut, CH-5232 Villigen PSI, Switzerland

⁶Dipartimento di Scienze Fisiche, Università “Federico II” di Napoli, Via Cintia I-80126 Napoli, Italy

(Received 12 January 2012; revised manuscript received 12 September 2012; published 15 October 2012)

An extensive surface characterization of hydrofluoric acid (HF) etched and annealed SrTiO₃ single crystals, vacuum-annealed below 300 °C, reveals the formation of a two-dimensional electron gas (2DEG). A joint scanning tunneling spectroscopy and low-energy electron diffraction analysis allows us to associate the surface metallic state (characterized by the presence of a nonzero density of states close to the Fermi level) with the low-temperature-annealed highly ordered 1 × 1 reconstructed SrTiO₃ surface hosting two-dimensional carriers. Meanwhile, a gap opens in the tunneling spectrum of 2 × 1 reconstructed, high-temperature-annealed surfaces. X-ray photoemission spectroscopy shows that the metallic state is associated with the surface formation of Ti³⁺. Recently published photoemission data demonstrated the formation of a 2DEG on the surface of cleaved SrTiO₃, while scanning tunneling spectroscopy on crystals heated at high temperature revealed gaplike features: Our results can help reconcile this seemingly contradicting phenomenology observed so far by scanning tunneling spectroscopy and photoemission spectroscopy.

DOI: [10.1103/PhysRevB.86.155425](https://doi.org/10.1103/PhysRevB.86.155425)

PACS number(s): 68.47.Gh, 73.20.-r, 87.64.Dz

I. INTRODUCTION

The formation of a two-dimensional electron gas (2DEG) at the interface between SrTiO₃ (STO) and LaAlO₃ (LAO) has attracted huge interest since its discovery¹ because of the intriguing functionalities related to this phenomenon, including high-electron mobility,² superconductivity,³ and possibly magnetism.^{4–7} The mechanism at the origin of the 2DEG formation is still the subject of much debate. Electronic reconstruction and charge transfer at the interface, in the “polar catastrophe” scenario, is arguably the most likely cause of the 2DEG formation,^{1,8–10} but oxygen vacancies and cation intermixing rearrangements at the interface have also been considered.^{11–16} The overall picture is clouded by the presence of several complicating factors, such as the possibility to have *n*- or *p*-type interfaces (according to the termination¹⁰), or the mixing between STO and LAO layers at the interface itself.¹⁷

While the formation of the 2DEG at the STO/LAO interface is now a well-accepted fact, it is not so obvious whether bare STO can exhibit the same phenomenon at its interface with vacuum. STO is the most popular substrate for epitaxial growth of functional oxides¹⁸ and superconducting thin films,^{19,20} and it is widely employed as a functional layer in all-oxide devices, such as superconducting field effect transistor^{21–23} and Josephson junctions.^{24,25} For these reasons, there is a tremendous interest in the study of its surface structural and electronic properties. Without the presence of the polar LaO and AlO₂ planes, an electronic reconstruction is not expected at the (001) surface of stoichiometric STO since the atomic planes are formally neutral. However, due to the partially covalent character of the cation-oxygen bonding, contrary to what the nominal charges of ions suggest, the SrO and

TiO₂ surfaces of STO are weakly polar, and thus they are subject to structural and possible electronic instabilities.²⁶ In addition, from an experimental point of view, while in LAO/STO a 2DEG at the interface is protected by the LAO overlayer, a free STO surface is in general unstable against structural and chemical reconstructions,^{27–31} and experiments must overcome this difficulty.

Very recent papers^{32,33} demonstrated the formation of a 2DEG on the surface of *in situ* cleaved STO by angle-resolved photoemission spectroscopy (ARPES). Oxygen vacancies, formed in the crystal fracturing³² or triggered by exposure to ultraviolet light,³³ have been indicated as responsible for the formation and confinement of the 2DEG seen by ARPES at the surface. Very interestingly, some of the electronic properties of the freshly cleaved surface are similar to those of the LAO/STO interface, and in particular they exhibit a similar splitting between *3d_{xy}* and *3d_{xz}/3d_{yz}* bands.^{12,34–36} On the other hand, scanning tunneling spectroscopy (STS) measurements on STO crystals heated at high temperature (on the order of 800–1200 °C) revealed gaplike features and several kinds of surface reconstruction.^{30,37,38} (Annealing is necessary to give conducting properties to a stoichiometric, insulating, STO crystal, making it suitable for STS measurements.) It has not yet been clarified whether the apparently opposite results between photoemission and tunneling analyses should be ascribed to possible differences in the techniques and in the physical phenomena that they probe (so that they can not really be compared), or instead are related to truly intrinsic differences in the samples due to the specific preparation procedures.

Here, we present the results of our investigation of the density of states (DOS) around the Fermi level by STS. The

samples were treated with different annealing procedures to produce conductivity at the surface. We found that thermal treatments on well-ordered TiO₂ surfaces at relatively low temperatures (250 °C) in ultrahigh-vacuum conditions create a surface layer hosting a 2D electron system. On the other hand, a treatment at higher temperature recovers the insulating surface state.

II. EXPERIMENT

STO crystals with (001) surface cut were purchased from SurfaceNet GmbH. Their surfaces were treated by a standard etching (in HF solution)³⁹ and annealing procedure at 950 °C, 1 h in oxygen (1 atm) under continuous flow (10³ sccm), to realize a TiO₂-terminated surface. Before being transferred *in situ* to the ultrahigh-vacuum (UHV) scanning tunneling microscope (STM) chamber (base pressure $\approx 5 \times 10^{-11}$ mbar), the samples were treated in oxygen atmosphere (0.1 mbar, 350 °C for 1 h). Further details regarding the sample preparation methods in our labs can be found in Ref. 40. The structural quality of the surface was checked by reflection high-energy electron diffraction (RHEED), which showed 1×1 diffraction patterns of the nonreconstructed (001) STO surfaces. The resulting STO crystals were transparent and any attempt to establish a tunnel current between the STM tip and the surface of such samples failed. On these insulating samples, as expected for stoichiometric STO without oxygen vacancies, atomic force microscope (AFM) images revealed the presence of atomically flat terraces [the mean roughness on the terrace being less than 0.1 nm, Fig. 1(a)], separated by single unit-cell steps. A detailed study of the quality of STO surfaces after identical treatment is reported in Ref. 41.

As opposed to the previously described process, the subsequent thermal treatments described in the next section resulted in conducting surfaces, which we explored by scanning tunneling microscopy and spectroscopy (STM/STS). The measurements were realized at room temperature using a commercial Omicron VT-AFM scanning tunneling microscope equipped with W or PtIr tips. Depending on the particular measurement, the tip-to-sample bias voltage (V_b) was set in

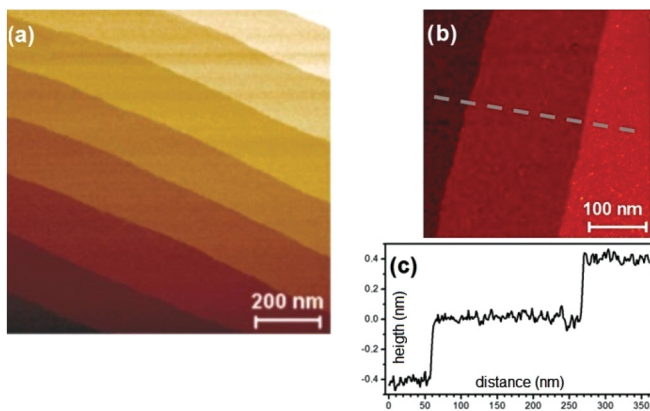


FIG. 1. (Color online) (a) Noncontact AFM topography ($1 \mu\text{m} \times 1 \mu\text{m}$) on a stoichiometric STO crystal showing the terrace structure of the surface. (b) STM topography ($400 \text{ nm} \times 400 \text{ nm}$) on Sample A (annealed at 250 °C), and (c) height profile along the shown dashed line.

the range of 1–2 V, with a tunneling current of 0.1–0.7 nA (tunneling resistance in the range of 1–20 G Ω).

III. TUNNEL RESULTS

Following the preliminary treatments to prepare the crystals, we first performed annealing at relatively low temperatures (i.e., in the range of 250–300 °C) and pressures of about 5×10^{-11} mbar. After these treatments, we observed by visual inspection that the samples remain transparent. However, as mentioned above, their surfaces were conducting, as revealed by the absence of charging effects (that are instead noticeable in fully oxidized samples) during low-energy electron diffraction (LEED). STM measurements also showed a difference: while it was impossible to get a tunneling current before the vacuum annealing treatment, stable tunnel junctions were established between the STM tip and the annealed surfaces. Figures 1(b) and 1(c) show an STM image of a sample annealed at 250 °C for 12 h in UHV conditions (Sample A), together with a height profile. These data demonstrate that high-surface quality was preserved in the annealed crystals, which is confirmed by the sharp 1×1 LEED patterns from these surfaces [Fig. 2(a)]. A thermal treatment at a slightly higher temperature of 350 °C (Sample B) did not change the morphology, and the LEED pattern remained the same. By contrast, a 2×1 reconstruction is observed on TiO₂-terminated STO annealed in vacuum at 900 °C [Sample C, Fig. 2(b)].

While in principle it is possible to obtain STM data with atomic resolution from samples that have been annealed at very high temperatures in UHV,^{27,30,42} attempts to achieve atomic resolution on our samples were unsuccessful. This is most likely due to the inherent difficulties to achieve suitable experimental conditions for this purpose on STO surface. Since the focus of this work is the study of STO surfaces annealed at lower temperatures, we did not attempt to reproduce STM images of conditions occurring at higher annealing temperatures, which have already been shown to include several types of reconstructions.^{30,42–45}

The tunneling current and differential tunneling conductance (by the standard lock-in technique; oscillation frequency and amplitude: 670 Hz, 20 mV) versus bias voltage (dI/dV curves) were recorded on Samples A, B, and C [Figs. 3(a) and 3(b)]. The curves were acquired over a grid of points on

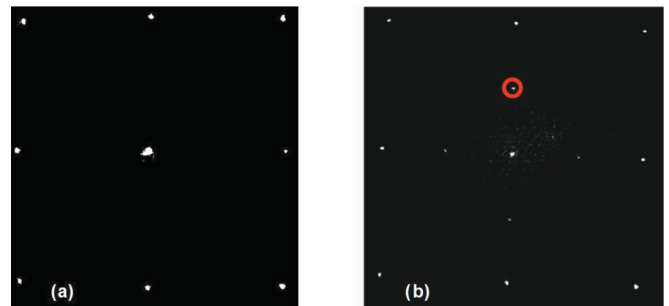


FIG. 2. (Color online) (a) LEED image on Sample A (annealed at 250 °C) exhibits a 1×1 pattern; the same result is obtained on Sample B (annealed at 350 °C). (b) On Sample C (annealed at 900 °C), the LEED pattern shows a 2×1 reconstruction of the surface.

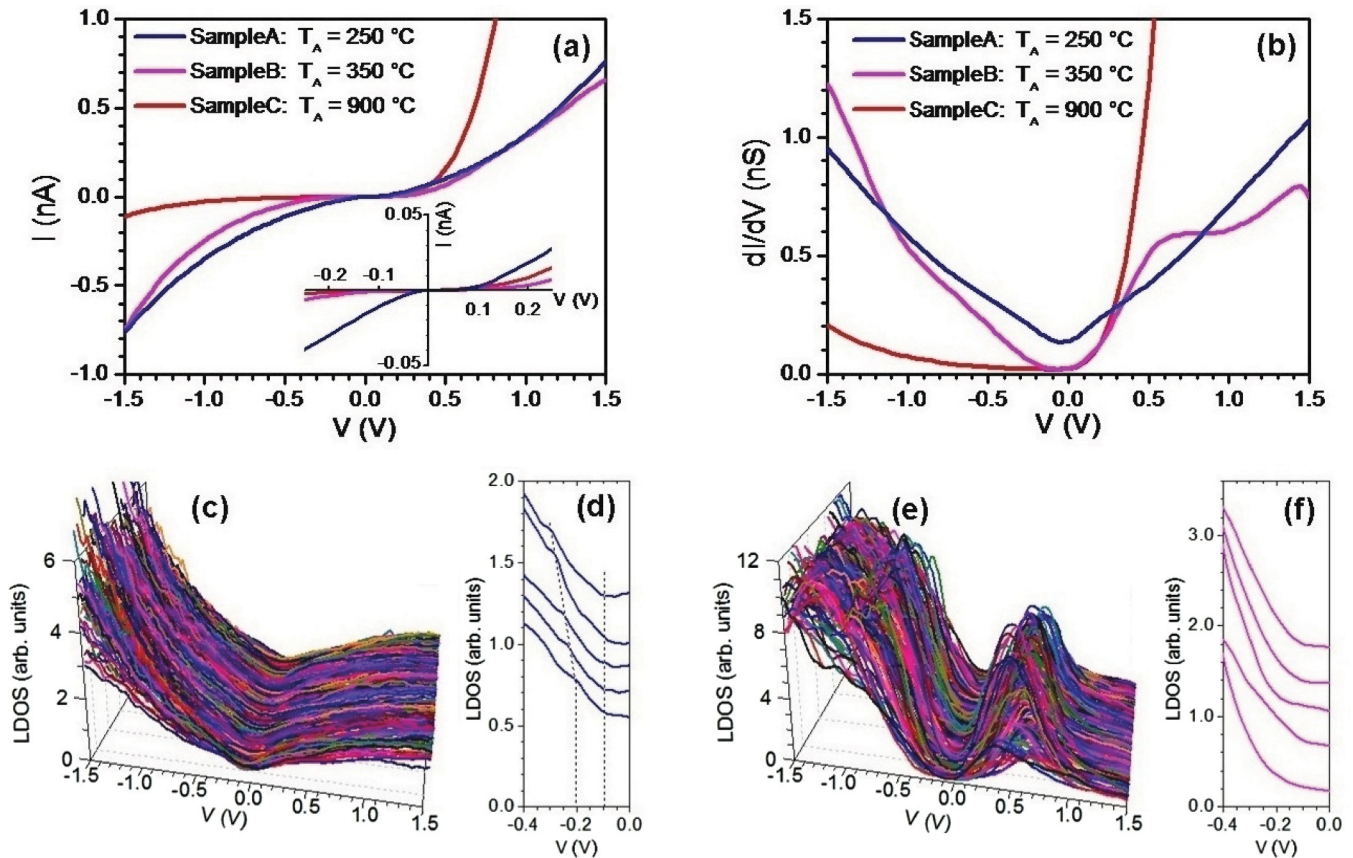


FIG. 3. (Color online) (a) Tunneling I - V (inset: magnification around $V = 0$) and (b) dI/dV recorded on Samples A, B, and C (T_A = annealing temperature). Tunneling curves were recorded at several locations on the surfaces forming a grid of point for each measured crystal, and the displayed curves are an average of all such single measurements. The tunneling conditions were $V_b = -1.5$ V, $I = 0.7$ nA for Samples A and B; $V_b = -1.5$ V, $I = 0.1$ nA for Sample C. (c) Tunneling DOS estimation for each measured curve using the normalization to the tunneling matrix coefficient for Sample A, as described in Ref. 46; (d) magnification of some DOS curves (vertically displaced for clarity) to highlight the spectroscopic structures described in the text. (e) and (f) Same DOS estimation, performed on Sample B.

several scanning regions in order to improve statistics and to check the homogeneity of the sample surface.

Bulk-conducting STO (Sample C) exhibits a strong asymmetry between occupied (negative bias) and unoccupied (positive bias) states and a quite flat near-zero signal below the Fermi energy. This behavior reflects the strongly asymmetric DOS of n -doped STO, where the doping promotes electrons into the empty Ti $3d$ states. At moderate doping, the Fermi level is not far from the bottom of the conduction band, which in stoichiometric bulk samples lies about 3.2 eV above the valence band edge. The donor states partially fall within the gap region, but the associated DOS is low. On this basis, a substantial flux of electrons from the metallic tip jumps into the free states above the Fermi level under positive bias, while the reverse process is dramatically hampered, resulting in diodelike I - V characteristics and corresponding dI/dV curves [Figs. 3(a) and 3(b)]. On the other hand, the low- T annealed Sample A (250 °C) shows very different STS spectra, which are unusual in many respects. The dI/dV spectra show nonzero conductivity at the Fermi level, an almost symmetric behavior at low bias for occupied and unoccupied states, and a V-shaped background. Sample B, which was annealed at a slightly higher temperature (350 °C),

shows instead a gaplike feature and low DOS at the Fermi level, suggesting this surface has a less metallic character, even if it does not yet exhibit the asymmetric fully gapped feature described for Sample C. Similar features were observed by STS on nonreconstructed TiO_2 -terminated STO,^{30,42} in agreement with *ab initio* calculations.³⁰

IV. DISCUSSION

While the observation on Sample C is not surprising, being consistent with previous tunneling measurements,^{30,42} it is remarkable to notice that vacuum annealing procedures at lower temperatures produce tunneling curves exhibiting more conductinglike appearances. These findings indicate different behaviors between the electronic features of the bulk and the surface as a consequence of thermal treatments in vacuum. Indeed, the visual inspection shows transparent bulk samples, which are therefore still insulating (and actually it is well known that such low-temperature annealings are not able to produce conducting samples). This means that the conducting or insulating character of the tunneling curves can not be ascribed to the bulk transport properties. Samples A and B have surfaces with conducting properties (as proven by the

appearance of the STS spectra), despite the fact that the annealing at temperatures below 400 °C are not able to produce a conducting state in the bulk (as it is, on the contrary, for Sample C); the spectroscopic conducting appearance of their surfaces can only be explained by assuming that the relatively significant amount of created free electrons are confined in a thin two-dimensional surface layer, enhancing the carrier density and, likely, resulting in a 2DEG state similar to what has been observed by ARPES on *in situ* cleaved STO.^{32,33} The dramatic difference between the electronic properties of the bulk and the surface is consistent with data reported in Ref. 33, where the features of the 2DEG on the STO surface are independent of the STO bulk properties over a large range of bulk carrier densities, from less than 10^{13} cm⁻³ (insulating STO) to 10^{20} cm⁻³ (strongly doped). We will focus later on possible interpretations of mechanisms leading to the 2DEG formation with moderate annealing, and why it looks less evident when slightly increasing the annealing temperature (Sample B) and can even be destroyed by higher temperatures (Sample C).

Some fine structures in the spectroscopic curves measured on Sample A also appear to be connected to the 2DEG state. We estimated the local density of states (LDOS) through a normalization procedure reviewed in Ref. 46 and references therein. The procedure is based on the normalization of the tunneling differential conductance curves to a tunneling matrix coefficient T in an algorithm also involving the I versus V curves. The coefficient T , depending on the (unknown) work functions of the electrodes and on the tip-to-sample separation, can be estimated through a fit of the dI/dV curve itself. This method provides a reliable estimation of the LDOS close to the Fermi energy. The details concerning the calculation procedure and the principles can be found in Ref. 46, as well as some cited examples of application of this procedure. In Fig. 3(c), we report the estimated LDOS curves for each surface location of Sample A (best fit parameters: tip-sample distance = 0.5 nm, work function = 4 eV), showing the high reproducibility of the results over the whole scanned area, while Fig. 3(d) highlights the spectroscopic features of the occupied states which can be compared with published ARPES results. The LDOS is characterized by a nonzero value at the Fermi energy, and by two reproducible structures at about -100 meV (where the DOS plateau near the Fermi level starts to increase) and between -200 and -300 meV (a pronounced kink whose energy position and appearance are slightly dependent on the location). For comparison, we also report in Figs. 3(e) and 3(f) the results of the same procedure applied to the tunneling spectra collected on Sample B: the curves are less homogeneous than on Sample A, the zero-bias LDOS is much lower, and the spectroscopic fine structures are much more smeared or even absent (depending on the location).

From theoretical calculations and recent ARPES measurements performed on freshly cleaved STO surfaces demonstrating the existence of a 2D electron system,^{32,33} one of the signatures of the 2DEG state is the presence of multiple metallic subbands (which are not expected for STO bulk samples) associated with a confining surface potential. The deepest of these bands extends between 200 and 300 meV below the Fermi level, while the next lowest band extends to about 100 meV below E_F . Our findings are consistent with

the results obtained by ARPES: the conductinglike spectra recorded on Sample A exhibit features at the same energy positions, while the spectra on Sample B lose such structures and move towards an insulating character, suggesting that the spectroscopic behavior of the surface is related to the 2DEG formation or disappearance.

The apparent reopening of a gaplike structure when the annealing temperature is increased indicates an evolution back to the insulating state. The apparent reopening of a gaplike structure when the annealing temperature is increased shows a nonmonotonic evolution of the surface DOS. Indeed, this occurrence indicates that the metalliclike spectra obtained after the lowest- T annealing are no longer preserved when the samples are heated at higher temperatures: the spectra recorded on Sample B and more evidently on Sample C tend to recover a DOS more similar to that of a stoichiometric crystal. Such nonmonotonic behavior might be due (at least in the low-temperature-annealing regime) to the competition of the thermal-activated oxygen fluxes from the bulk to the surface and from the surface to the vacuum, resulting in an increase of the surface disorder. Alternatively or in addition, as a consequence of increasing annealing temperature in the low-temperature regime, the surface might be degraded by the diffusion of oxygen or cationic species to the surface (as observed, for example, in Ref. 47), or be affected by structural distortions. High-temperature annealing, on the other hand, produces a new kind of ordered surface (1×2) (Sample C) caused by a higher depletion of the oxygen.

Data from x-ray photoemission spectroscopy (XPS) indicate a difference in the photoemission signal coming from spectroscopic features attributed to Ti^{3+} between spectra collected on samples annealed below 400 °C (such as Samples A and B) and samples annealed at higher temperatures (such as Sample C). Figure 4 shows XPS spectra from Samples A and C around the binding energies of the Ti $2p$ doublet states (photon energy: $h\nu = 1.119$ keV) at emission angles from the STO surface of $\theta = 55^\circ$ (i.e., shallow emission 35° off-normal from the STO surface plane). This configuration of the measurement enhances the surface sensitivity. The shoulder at the lower binding-energy side, located between 457 and 458 eV, is routinely attributed to the presence of Ti^{3+} states,⁴⁸ rather than the Ti^{4+} states of bulk stoichiometric STO. The Ti^{3+} detection only when the system exhibits

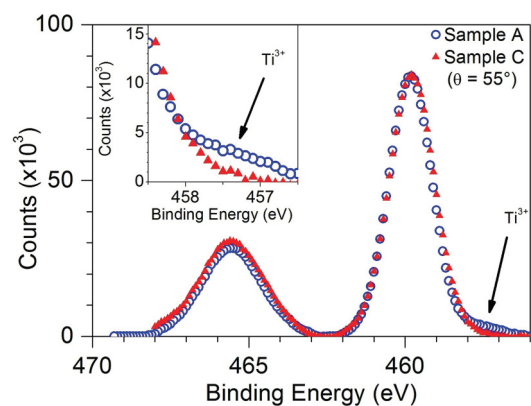


FIG. 4. (Color online) XPS spectra on Samples A and C around the binding energy range of the Ti $2p$ doublet states.

surface metallicity supports the hypothesis that the oxygen vacancies concentration at the surface (even in a state in which the bulk can not have a large vacancies concentration) could be responsible of the observed conductinglike tunnel spectra, by increasing the electron density around Ti sites. The spectra collected on Sample C under the same conditions do not show a pronounced Ti^{3+} shoulder, despite the fact that Sample C, with its 1×2 reconstructed surface, should have higher concentration of surface and bulk oxygen vacancies in comparison to Samples A and B. The relative lack of Ti^{3+} seen by XPS at the surface of Sample C is consistent with its insulating nature and suggests that structural reconstruction (e.g., vacancy ordering) and/or disorder (e.g., Sr migration) along with associated band-bending effects³² induced during the annealing process can kill the metallic surface state found at lower annealing temperatures.

V. CONCLUSIONS

In conclusion, we measured the tunneling DOS of TiO_2 -terminated STO single crystals after annealing in UHV at different temperatures. In the resulting noninsulating surface state, the presence of a nonzero DOS above and below the Fermi level was observed after thermal treatments at relatively low temperatures. The interpretation in terms of

2D confinement of carriers is supported by the experimental evidences, and by some spectroscopic features in agreement with very recent ARPES measurements on vacuum-cleaved STO, which showed the presence of a 2DEG at the surface. The existence of an optimal temperature for the observation of the effect could be explained in terms of competition between the oxygen diffusion from the bulk to the surface and the oxygen loss from the surface to the vacuum. Alternatively, or in addition, careful low-temperature annealing may induce surface structural changes consistent with 1×1 surface ordering (such as Ti-O bond buckling) which could play a role in 2DEG formation. Further increasing the annealing temperature eventually leads to the complete disappearance of the 2DEG, and it is possible that additional effects aside from the oxygen dynamics at the surface are responsible for this behavior.

ACKNOWLEDGMENTS

The research leading to these results has received funding from the European Union Seventh Framework Programme (FP7/2007-2013) under Grant Agreement No. 264098-MAMA. M.R. and Z.R. acknowledge the support of the Ministry of Education and Science of the Republic of Serbia (Project No. OI-171023).

*rdicapua@na.infn.it

†milan.radovic@epfl.ch

¹A. Othomo and H. Y. Hwang, *Nature (London)* **427**, 423 (2004).

²B. Jalan, S. J. Allen, G. E. Beltz, P. Moetakef, and S. Stemmer, *Appl. Phys. Lett.* **98**, 132102 (2011).

³N. Reyren, S. Thiel, A. D. Caviglia, L. F. Kourkoutis, G. Hammerl, C. Richter, C. W. Schneider, T. Kopp, A.-S. Rüetschi, D. Jaccard, M. Gabay, D. A. Muller, J.-M. Triscone, and J. Mannhart, *Science* **317**, 1196 (2006).

⁴A. Brinkman, M. Huijben, M. van Zalk, J. Huijben, U. Zeitler, J. C. Maan, W. G. van der Wiel, G. Rijnders, D. H. A. Blank, and H. Hilgenkamp, *Nat. Mater.* **6**, 493 (2007).

⁵Ariando, X. Wang, G. Baskaran, Z. Q. Liu, J. Huijben, J. B. Yi, A. Annadi, A. R. Barman, A. Rusydi, S. Dhar, Y. P. Feng, H. H. J. Ding, and T. Venkatesan, *Nat. Commun.* **2**, 188 (2011).

⁶L. Li, C. Richter, J. Mannhart, and R. C. Ashoori, *Nat. Phys.* **7**, 762 (2011).

⁷J. A. Bert, B. Kalisky, C. Bell, M. Kim, Y. Hikita, H. Y. Hwang, and K. A. Moler, *Nat. Phys.* **7**, 767 (2011).

⁸C. Cantoni, J. Gazquez, F. Miletto Granozio, M. P. Oxley, M. Varela, A. R. Lupini, S. J. Pennycook, C. Aruta, U. Scotti di Uccio, P. Perna, and D. Maccariello, *Adv. Mater.* **24**, 3952 (2012).

⁹G. Singh-Bhalla, C. Bell, J. Ravichandran, W. Siemons, Y. Hikita, S. Salahuddin, A. F. Hebard, H. Y. Hwang, and R. Ramesh, *Nat. Phys.* **7**, 80 (2011).

¹⁰N. Nakagawa, H. Y. Hwang, and D. A. Muller, *Nat. Mater.* **5**, 204 (2006).

¹¹S. A. Chambers, *Surf. Sci.* **605**, 1133 (2011).

¹²K.-J. Zhou, M. Radovic, J. Schlappa, V. Strocov, R. Frison, J. Mesot, L. Patthey, and T. Schmitt, *Phys. Rev. B* **83**, 201402 (2011).

¹³S. Chambers, M. Engelhard, V. Shutthanandan, Z. Zhu, T. Droubay, L. Qiao, P. Sushko, T. Feng, H. Lee, T. Gustafsson, E. Garfunkel, A. Shah, J.-M. Zuo, and Q. Ramasse, *Surf. Sci. Rep.* **65**, 317 (2010).

¹⁴J. N. Eckstein, *Nat. Mater.* **6**, 473 (2007).

¹⁵G. Herranz, M. Basletic, M. Bibes, C. Carretero, E. Tafra, E. Jacquet, K. Bouzehouane, C. Deranlot, A. Hamzic, J.-M. Broto, A. Barthelemy, and A. Fert, *Phys. Rev. Lett.* **98**, 216803 (2007).

¹⁶P. R. Willmott, S. A. Pauli, R. Herger, C. M. Schlepütz, D. Martoccia, B. D. Patterson, B. Delley, R. Clarke, D. Kumah, C. Cionca, and Y. Yacoby, *Phys. Rev. Lett.* **99**, 155502 (2007).

¹⁷S. A. Pauli, S. J. Leake, B. Delley, M. Björck, C. W. Schneider, C. M. Schlepütz, D. Martoccia, S. Paetel, J. Mannhart, and P. R. Willmott, *Phys. Rev. Lett.* **106**, 036101 (2011).

¹⁸M. Radovic, M. Salluzzo, Z. Ristic, R. Di Capua, N. Lampis, R. Vaglio, and F. Miletto Granozio, *J. Chem. Phys.* **135**, 034705 (2011).

¹⁹F. Tafuri, J. R. Kirtley, D. Born, D. Stornaiuolo, P. G. Medaglia, P. Orgiani, G. Balestrino, and V. G. Kogan, *Europhys. Lett.* **73**, 948 (2006).

²⁰R. Vaglio, M. G. Maglione, and R. Di Capua, *Supercond. Sci. Technol.* **15**, 1236 (2002).

²¹A. Cassinese, G. M. De Luca, A. Prigiobbo, M. Salluzzo, and R. Vaglio, *Appl. Phys. Lett.* **84**, 3933 (2004).

²²M. Salluzzo, G. Ghiringhelli, J. C. Cezar, N. B. Brookes, G. M. De Luca, F. Fracassi, and R. Vaglio, *Phys. Rev. Lett.* **100**, 056810 (2008).

²³M. Salluzzo, A. Gambardella, G. M. De Luca, R. Di Capua, Z. Ristic, and R. Vaglio, *Phys. Rev. B* **78**, 054524 (2008).

²⁴D. Stornaiuolo, G. Rotoli, K. Cedergren, D. Born, T. Bauch, F. Lombardi, and F. Tafuri, *J. Appl. Phys.* **107**, 11390 (2010).

- ²⁵L. Longobardi, D. Massarotti, D. Stornaiuolo, L. Galletti, G. Rotoli, F. Lombardi, and F. Tafuri, *Phys. Rev. Lett.* **109**, 050601 (2012).
- ²⁶R. I. Eglitis and D. Vanderbilt, *Phys. Rev. B* **77**, 195408 (2008).
- ²⁷M. R. Castell, *Surf. Sci.* **516**, 33 (2002).
- ²⁸G. Charlton, S. Brennan, C. A. Muryn, R. McGrath, D. Norman, T. S. Turner, and G. Thornton, *Surf. Sci.* **457**, L376 (2000).
- ²⁹Q. D. Jiang and J. Zegenhagen, *Surf. Sci.* **425**, 343 (1999).
- ³⁰T. Kubo and H. Nozoye, *Surf. Sci.* **542**, 177 (2003).
- ³¹M. Radovic, N. Lampis, F. Miletto Granozio, P. Perna, Z. Ristic, M. Salluzzo, C. M. Schleputz, and U. Scotti di Uccio, *Appl. Phys. Lett.* **94**, 022901 (2009).
- ³²A. F. Santander-Syro, O. Copie, T. Kondo, F. Fortuna, S. Pailhes, R. Weht, X. G. Qiu, F. Bertran, A. Nicolaou, A. Taleb-Ibrahimi, P. L. Fevre, G. Herranz, M. Bibes, N. Reyren, Y. Apertet, P. Lecoeur, A. Barthelemy, and M. J. Rozenberg, *Nature (London)* **469**, 189 (2011).
- ³³W. Meevasana, P. D. C. King, R. H. He, S.-K. Mo, M. Hashimoto, A. Tamai, P. Songsiriritthigul, F. Baumberger, and Z.-X. Shen, *Nat. Mater.* **10**, 114 (2011).
- ³⁴M. Salluzzo, J. C. Cezar, N. B. Brookes, V. Bisogni, G. M. De Luca, C. Richter, S. Thiel, J. Mannhart, M. Huijben, A. Brinkman, G. Rijnders, and G. Ghiringhelli, *Phys. Rev. Lett.* **102**, 166804 (2009).
- ³⁵Z. Ristic, R. Di Capua, G. M. De Luca, F. Chiarella, G. Ghiringhelli, J. C. Cezar, N. B. Brookes, C. Richter, J. Mannhart, and M. Salluzzo, *Europhys. Lett.* **93**, 17004 (2011).
- ³⁶Z. Ristic, R. Di Capua, F. Chiarella, G. M. De Luca, I. Maggio-Aprile, M. Radovic, and M. Salluzzo, *Phys. Rev. B* **86**, 045127 (2012).
- ³⁷F. Silly, D. T. Newell, and R. Castell, *Surf. Sci.* **600**, L219 (2006).
- ³⁸R. Shimizu, K. Iwaya, T. Ohsawa, S. Shiraki, T. Hasegawa, T. Hashizume, and T. Hitosugi, *Appl. Phys. Lett.* **100**, 263106 (2012).
- ³⁹M. Kawasaki, K. Takahashi, T. Maeda, R. Tsuchiya, M. Shinohara, O. Ishiyama, T. Yonezawa, M. Yoshimoto, and H. Koinuma, *Science* **266**, 1540 (1994).
- ⁴⁰M. Radovic, Ph.D. thesis, Universita degli Studi di Napoli Federico II, Italy, 2008, see <http://www.fedoa.unina.it/3474/>.
- ⁴¹A. Fragneto, G. M. De Luca, R. Di Capua, U. Scotti di Uccio, M. Salluzzo, X. Torrelles, T. L. Lee, and J. Zegenhagen, *Appl. Phys. Lett.* **91**, 101910 (2007).
- ⁴²H. Tanaka, T. Matsumoto, T. Kawai, and S. Kawai, *Jpn. J. Appl. Phys.* **32**, 1405 (1993).
- ⁴³D. S. Deak, F. Silly, K. Porfyrakis, and M. R. Castell, *Nanotechnology* **18**, 075301 (2007).
- ⁴⁴D. T. Newell, A. Harrison, F. Silly, and M. R. Castell, *Phys. Rev. B* **75**, 205429 (2007).
- ⁴⁵Z. Wang, K. Wu, Q. Guo, and J. Guo, *Appl. Phys. Lett.* **95**, 021912 (2009).
- ⁴⁶M. Passoni, F. Donati, A. Li Bassi, C. S. Casari, and C. E. Bottani, *Phys. Rev. B* **79**, 045404 (2009).
- ⁴⁷F. Silly and R. Castell, *Appl. Phys. Lett.* **85**, 3223 (2004).
- ⁴⁸E. Frantzeskakis, J. Avila, and M. C. Asensio, *Phys. Rev. B* **85**, 125115 (2012).